INTERNATIONAL JOURNAL OF CLIMATOLOGY
Int. J. Climatol. **37**: 4486–4492 (2017)
Published online 3 May 2017 in Wiley Online Library
(wileyonlinelibrary.com) DOI: 10.1002/joc.5085

RMetS
Royal Meteorological Society

Short Communication

Characterization of convective systems and their association with African easterly waves

Hilawe Semunegus,[a,b]* Ademe Mekonnen[b] and Carl J. Schreck III[a,b,c]
[a] *NOAA's National Centers for Environmental Information (NCEI), Asheville, NC, USA*
[b] *Energy and Environmental Systems Department, North Carolina A&T State University, Greensboro, NC, USA*
[c] *Cooperative Institute for Climate and Satellites – NC (CICS-NC), North Carolina State University, Asheville, NC, USA*

ABSTRACT: This study investigates the relationship between African easterly waves (AEWs) and different types of deep convection. It is known that AEWs impact the development of deep convection over tropical North Africa and tropical cyclone formation over the eastern Atlantic. However, the process of how AEWs interact with deep convection is not well understood. Composite analysis based on a 24-year data set of cloud systems (CS) from the International Satellite Cloud Climate Project shows that the relationship changes with various types of convection over this region. This phase change relationship analysis may shed light into the dynamics of AEWs and improve the ability of forecasters to anticipate associated rainfall over the Sahel. Weak and disorganized convective systems (WDCSs; 50 km < radius < 100 km) are most common within the southerly phase of the AEWs over East Africa. Mesoscale convective systems (MCSs) with cloud radii >100 km increase in frequency within and to the west of the AEW-trough zone. MCSs are common features of summer in northwestern Africa. Our results indicate that the association between AEWs and deep convection is different and changes across North Africa. Weak AEWs over East Africa have a stronger relationship with WDCSs, while mature AEWs over West Africa have more MCS activity. This evolution suggests that the organization of convection from WDCS to MCS may play a critical role in AEW development. This hypothesis contrasts the traditional view that treats convection uniformly.

KEY WORDS African easterly waves; AEW; convective systems; African easterly jet; ISCCP

Received 27 June 2016; Revised 13 February 2017; Accepted 13 March 2017

1. Introduction

A substantial part of moist convection in the Tropics is associated with wave disturbances. Over tropical North Africa, e.g. African easterly waves (AEWs) modulate deep convection and rainfall on daily timescales (Carlson, 1969; Fink and Reiner, 2003). AEWs explain about 30–35% of the total convective variance over tropical Africa and more than 40% over the eastern Atlantic during boreal summer (Mekonnen *et al.*, 2006).

Despite several decades of research, the initiation and variability of AEWs, including their interaction with convective activity, remains an active area of investigation. Early studies showed that AEWs are initiated in association with an unstable midlevel African easterly jet (AEJ), a prominent weather system of the African summer monsoon (Burpee, 1972; Norquist *et al.*, 1977; Reed *et al.*, 1977; Thorncroft and Hoskins, 1994). However, the AEJ may be only marginally unstable, as suggested by Hall *et al.* (2006) and Thorncroft *et al.* (2008). In a series of papers, Hsieh and Cook (2005, 2007, 2008) provided evidence that the AEJ presence is not a necessary condition for AEW initiation and that convection could be the generating mechanism for AEWs. Other studies (Carlson, 1969; Berry and Thorncroft, 2005; Lin *et al.*, 2005; Mekonnen *et al.*, 2006) also show evidence that AEW initiation over East Africa cannot be explained by the presence of a midlevel jet but are likely initiated by pre-existing convective activity.

Many studies have related Atlantic tropical cyclone (TC) formation with AEWs that propagate off the coast of West Africa. Recent studies extend the relationship further, finding that most AEWs, especially those that spawn TCs, originated near the Ethiopian highlands of East Africa (Lin *et al.*, 2005). Even so, less attention has been given to AEWs over East Africa compared with AEW activity near the West African coast. This underscores the importance of expanding research and knowledge to include the central and eastern part of the African continent during boreal summer.

Mesoscale convective systems (MCSs) constitute the largest contribution to rainfall in tropical Africa during boreal summer (Hodges and Thorncroft, 1997; Mathon and Laurent, 2001). Most MCSs are generated orographically (Laing and Fritsch, 1993), but MCSs over North

* Correspondence to: H. Semunegus, NOAA's National Centers for Environmental Information (NCEI), 151 Patton Ave., Asheville, NC 28801-5001, USA. E-mail: Hilawe.Semunegus@noaa.gov

Africa are also generated in association with AEWs (Fink and Reiner, 2003). The relative importance of orography and AEWs for the organization and lifecycle of MCSs over North Africa remains unclear. While the relationship between AEW and convection has been relatively well documented in West Africa, the processes that determine how propagating AEWs impact MCSs and squall lines over central and eastern regions in North Africa are not well understood.

Mekonnen and Rossow (2011) used a combination of satellite observations and reanalysis data to characterize different types of convective activities and their relationships with AEWs in East Africa. They found that weak and disorganized convective systems (WDCSs) propagate westward from the Arabian Sea and western Indian Ocean and transition to MCSs west of the Ethiopian highlands.

This study provides a climatological perspective as to how convection interacts with AEWs across North Africa during the summer [July–September (JAS)] season. Studies have shown that different types of cloud systems are associated with different types of precipitation (Rossow *et al.*, 2012) and have different radiative effects (Oreopoulos and Rossow, 2011). In this work, we use the Convective Systems (CS) data set (Machado *et al.*, 1998) from International Satellite Cloud Climatology Project (ISCCP) to expand on past work (Mekonnen and Rossow, 2011) that exhibit relationships between AEWs, MCSs, and WDCSs between East and West Africa.

2. Data and methods

2.1. ISCCP convective system data

ISCCP provides various satellite-observed cloud data sets that sample at intervals of 3-h and about 30 km from geostationary and polar orbiting satellites (Rossow and Schiffer, 1999). In this study we use the ISCCP CS data, which dates to July 1983. The CS data set is used to distinguish different types of deep convective states for the Americas (Machado *et al.*, 1998). CSs are identified by a contiguous region of cloudy pixels that contain clouds in the upper troposphere and determined by infrared brightness temperature of cold cloud tops <245 K. A further analysis of convective cloud tops <220 K identifies convective clusters (CC) in CS in each geostationary satellite at 3-h intervals. The CSs represent all high-level cloud systems and deep convective towers that are described by location, size, shape, etc., including MCSs (see Machado and Rossow, 1993). CS data include information about cold cloud size and cloud properties, including small (down to 17 km) and scattered convection. As described in Machado *et al.* (1998), the CS size is reported as the radius (km) of a circle with the same area as covered by the image pixels composing the CS, i.e. radius, $r = \sqrt{N\frac{A}{\pi}}$, where N is number of pixels and A is the area of pixel. Thus, a linear squall line and a circular MCS of the same area would have the same radius. The difference between them is described in the CS data by their eccentricity, but that variable is not used in the current analysis. More details of ISCCP CSs can be found in Machado *et al.* (1998), Rossow *et al.* (1996), and Machado and Rossow (1993) and online at http://isccp.giss.nasa.gov/CT/.

The ISCCP CS data were binned and totaled for the study period and location in order to form composites (explained in Section 2.2) and climatological analysis. In this study, MCSs are defined as CSs with radii >100 km, mean cloud temperature <245 K for the entire convective system, and with at least one overshooting top (CC < 220 K) (Maddox, 1980; Machado and Rossow, 1993; Machado *et al.*, 1998; Carvalho and Jones, 2001). This definition closely matches the classic MCS definition of Maddox (1980). Smaller CS that fall between 50 and 100 km and have cloud temperatures <245 K are categorized as WDCSs. The WDCS are the most frequent convective system in the Tropics (see Figure 1; Rossow *et al.*, 2005; Rossow *et al.*, 2013; Tan *et al.*, 2013).

2.2. ECMWF-Interim reanalysis data

The ERA-Interim reanalysis data set was used for describing atmospheric states and dynamical fields (Simmons *et al.*, 2007). ERA-Interim is available at 6-h, 0.75° horizontal grid, and 37 pressure levels for the period 1979–present. For this study, 700-mb level daily averages of meridional winds were used.

2.3. Analysis methods

Previous studies frequently identify AEWs by filtering variables like meridional wind or convective proxies for the typical temporal and/or spatial scales of AEWs. In this study, we identified the waves by filtering 700-hPa meridional wind from ERA-Interim (Simmons *et al.*, 2007) for periods of 2.5–10 days and westward propagating zonal wavenumbers 0–20. Kiladis *et al.* (2006) examined AEWs with a somewhat narrower version of this to filter outgoing longwave radiation. The results are generally insensitive to the details of the filtering technique. However, the inclusion of zonal wavenumber filtering is useful over East Africa where AEWs are generally weaker and may be obscured by stationary signals.

Composite anomalies were used to analyse the spatial characteristics and evolution of AEWs during JAS 1984–2007. Dates when the filtered meridional wind time series at a given location were >2 standard deviations (σ) were selected for the analysis. For the composites, meridional wind anomalies were calculated by simply subtracting the daily climatological mean. CS anomalies, on the other hand, were determined by subtracting the mean for lags −6 to +6 days at each latitude/longitude bin.

3. Results

3.1. General convection type phases over East and West Africa

Figure 1 shows the 1° latitude–longitude frequency of CSs over tropical Africa for JAS 1984–2007. MCSs are most common over the high terrain in eastern, central, and western Africa, consistent with highest rainfall (Janiga

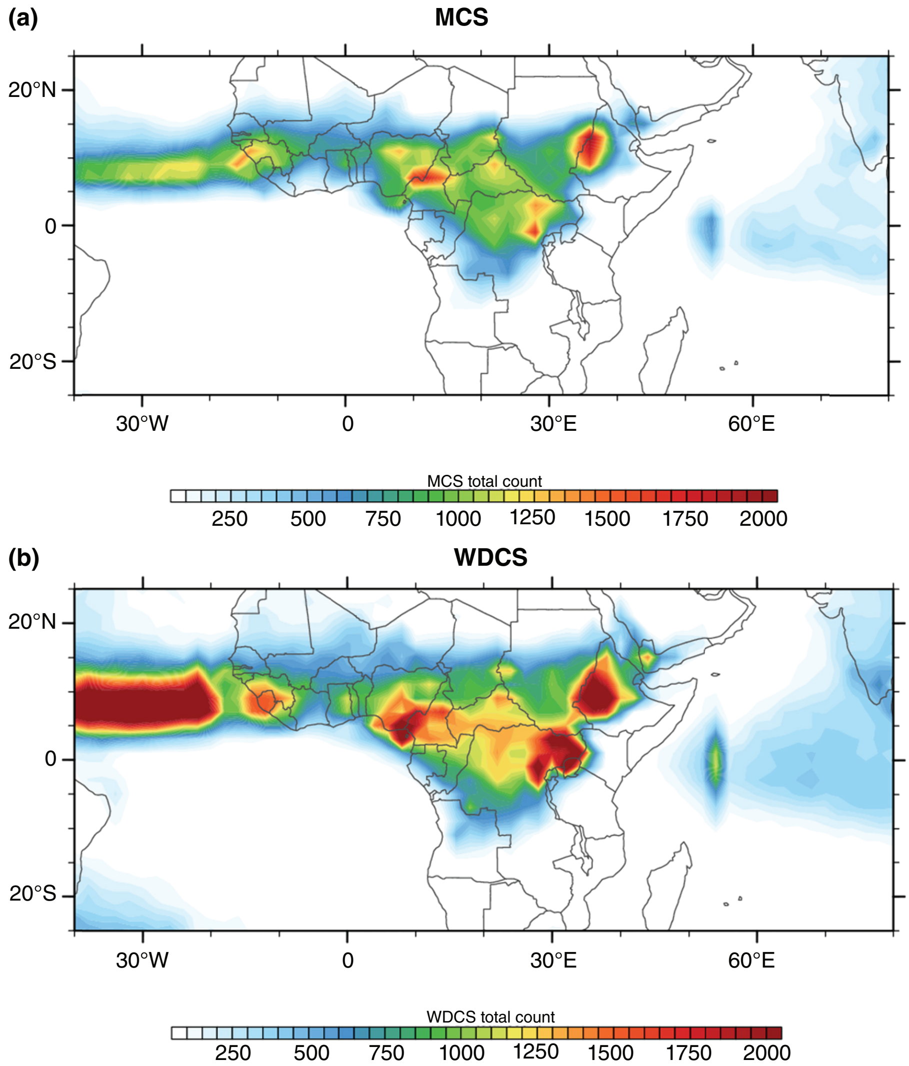

Figure 1. Frequency of occurrences of ISCCP Convective Systems (1° binned counts; shaded) of (a) MCS and (b) WDCS using the data set during July–September 1984–2007.

and Thorncroft, 2013; Novella and Thiaw, 2013). The CS-based MCS climatology agrees well with the frequency of deep and long-lived cloud regimes shown in Mekonnen and Rossow (2011). Figure 1(b) shows WDCS, which are CSs < 245 K and radius between 50 and 100 km. WDCS occurrences are detected over larger areas of North Africa compared with MCSs. The geographical distribution of the WDCSs is similar with isolated convective cloud types as seen in Mekonnen and Rossow (2011). Mekonnen and Rossow (2011) used a statistically derived data set but still showed a strong climatological agreement with the more objectively defined ISCCP CS data set.

The pattern and coverage of MCS and WDCS counts seen in Figure 1 strongly resemble the African rainfall JAS climatology (Janiga and Thorncroft, 2013; Novella and Thiaw, 2013) with maximum counts coinciding with peak rainfall areas. Rossow *et al.* (2013) show that larger and long-lived weather systems (such as MCSs) account for most of the heavy precipitation over the Tropics even though they are infrequent. In contrast, WDCSs account for most of the convective clouds in the Tropics (note higher frequencies in Figures 1(b) than (a)) but contribute little to heavy precipitation (Tromeur and Rossow, 2010). WDCS are also dominant over the North Atlantic Intertropical Convergence Zone (ITCZ) where maritime shallow convection is prevalent (Figure 1(b)).

3.2. Temporal phase evolution of convection and meridional winds

Figure 2 shows composite Hovmöllers of anomalous MCS and WDCS frequencies (anomalies are with respect to the 13-day mean; see Section 2.3 for description), associated with AEWs using a basepoint in West Africa (10°N, 0°). MCSs are more frequent at or ahead of the trough, while fewer MCSs occur near the ridge (Figure 2(a)). WDCSs are generally located behind the trough axis inside the southerlies, while they are suppressed in the northerly anomalies (Figure 2(b)). For both MCSs and WDCSs, their relationships with the AEWs are coherent from at least 20°E–20°W.

Figure 3 shows similar composites as in Figure 2, but for a basepoint in East Africa (12.5°N, 30°E). The AEWs

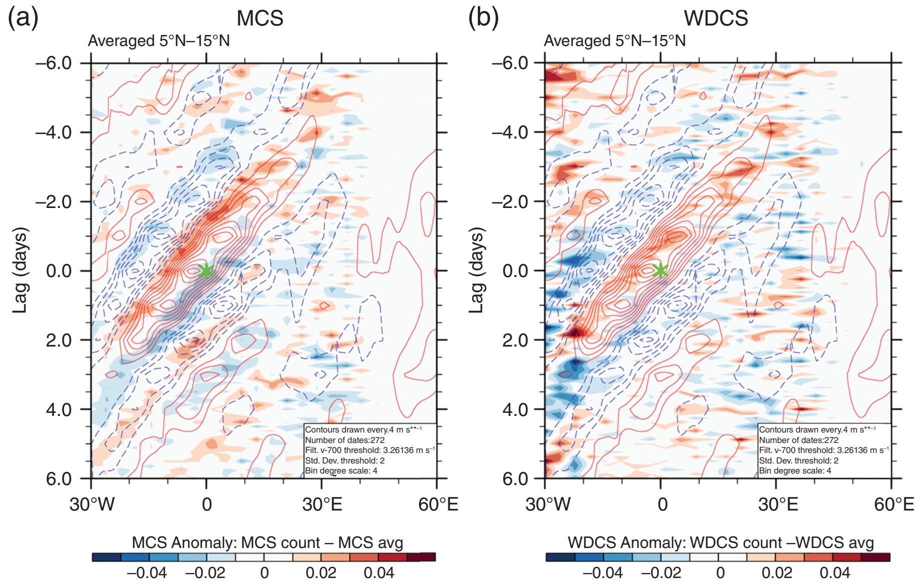

Figure 2. Hovmöller representation of easterly waves and associated (a) MCS and (b) WDCS binned count anomalies (shaded) at the nominal West African basepoint of 10.0°N, 0°E. Contours are unfiltered v-700 mb anomalies associated with the 2–10 day filtered v-700 mb basepoint time series with southerly (northerly) wind depicted in red (blue) contours. Basepoint centres are denoted by green asterisks. Shown are latitudinal averages between 5° and 15°N.

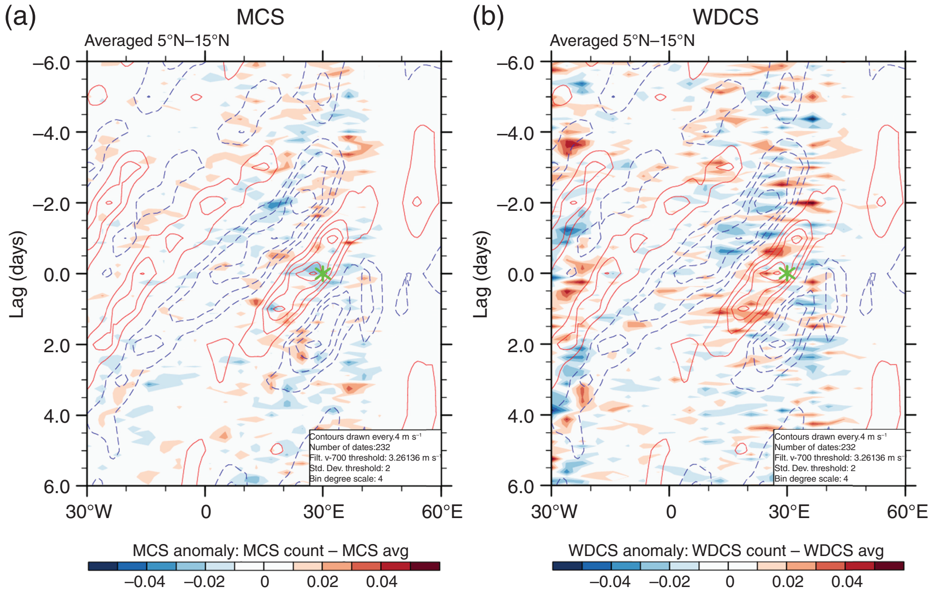

Figure 3. Hovmöller representation of easterly waves and associated (a) MCS and (b) WDCS binned count anomalies (shaded) at the nominal East African basepoint of 12.5°N, 30°E. Contours are unfiltered v-700 mb anomalies associated with the 2–10 day filtered v-700 mb basepoint time series with southerly (northerly) wind depicted in red (blue) contours. Basepoint centres are denoted by green asterisks. Shown are latitudinal averages between 5° and 15°N.

are significantly weaker than in Figure 2 because AEWs are at their formative stage in this region. Figure 3(a) also shows modulation of MCSs by AEWs but not as strongly as the West African equivalent (Figure 2(a)). The MCSs are enhanced in some parts of the southerlies and suppressed in others. The most dominant signal for MCSs is a stationary modulation in the vicinity of the Darfur Mountains (~20°E) around day +2. WDCSs, on the other hand, are enhanced within the southerlies between the trough and ridge axes (Figure 3(b)).

3.3. Characterizing convection phase changes in association with easterly wave genesis and intensification

Figure 4 shows the evolution of MCS (left) and WDCS (right) based on composites using AEW southerlies >2.0 σ at basepoints every 5° from 35° to 10°E. MCSs tend to be enhanced in the trough, particularly over West Africa (Figure 4(a)). This MCS and trough relationship is weaker at the 35° and 30°E basepoints where AEWs are at their initial stages, consistent with Figure 3(a). A red arrow tracked MCS development at 5° basepoint

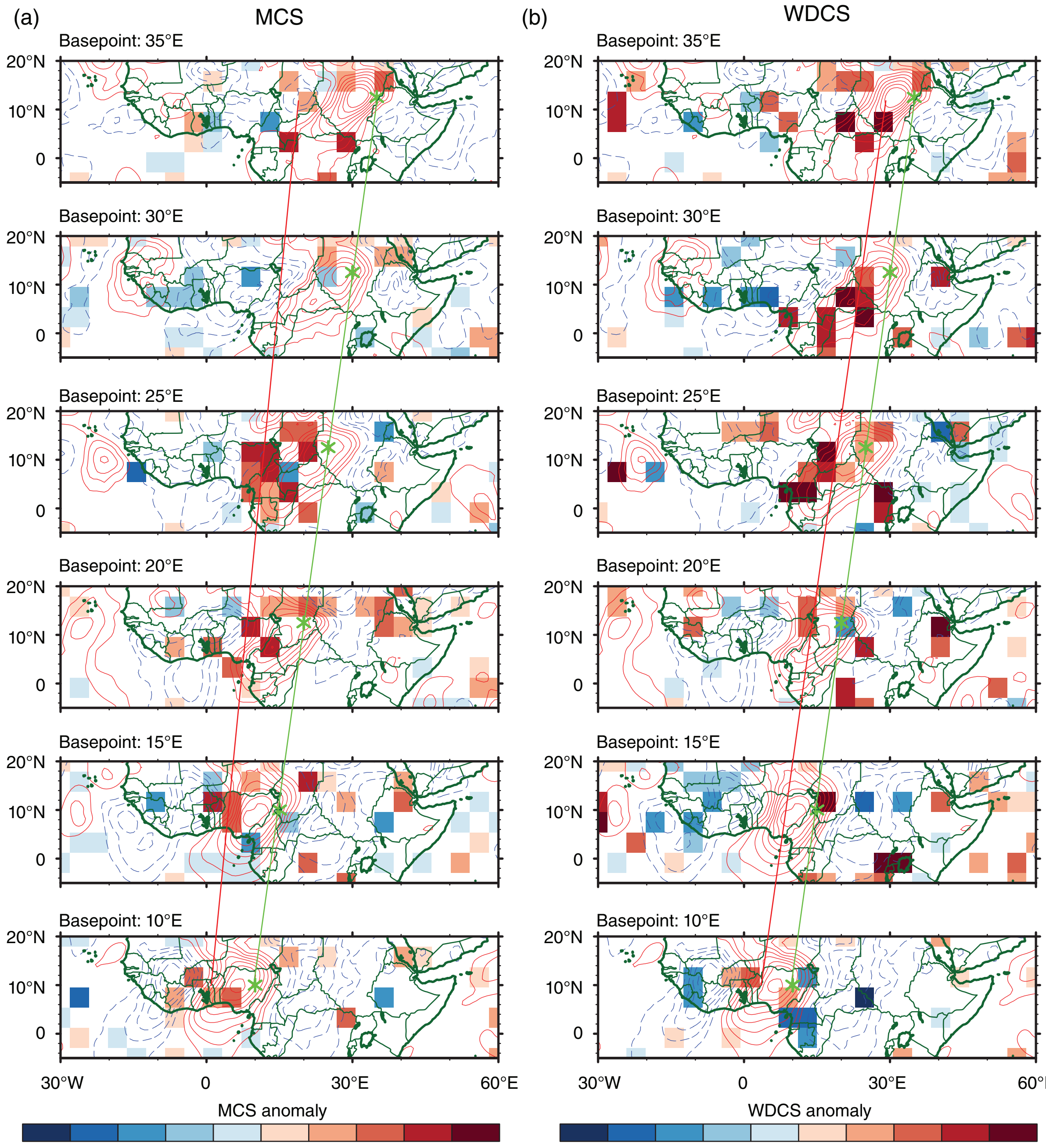

Figure 4. Basepoint tracking of (a) MCS and (b) WDCS binned count anomalies from 12.5°N, 35°E–10°N, 10°E. Contours are unfiltered v-700 mb anomalies associated with the 2–10 day filtered v-700 mb basepoint time series with southerly (northerly) wind depicted in red (blue) contours. The red arrow tracks the area of enhanced MCS and WDCS convection near the basepoints. The green arrow tracks the basepoint locations. Ninety percent (double sided) statistical significance has been applied.

intervals (westward) for comparison with wave phases, which is consistent with westward propagation shown in Figures 2(a) and 3(a). Starting at 25°E, strong coherent propagation between the MCS activity and AEWs is seen. For the 35°E basepoint, there is an area of enhanced MCS at 12°N, 20°E, at and ahead of the weak trough. MCSs are not clear at the 30°E basepoint but at the 25°E basepoint, enhanced MCS area expands into the trough of the southerly wave at and west of 12°E. The enhanced MCS shifts gradually toward the trough axis and extends slightly to the northerly wave at the 20°E basepoint. The organization of MCSs increases leading up to 10°E where the enhanced convection is located at the trough, characteristic of AEWs over West Africa (Reed *et al.*, 1977; Janiga and Thorncroft, 2016).

Consistent with Figures 2(b) and 3(b), WDCS tend to be enhanced in the AEW southerlies. For the 35°E basepoint (Figure 4, top-right), a small area of enhanced WDCS in the southerlies lies near 12°N, 30°E. It grows and organizes at the 30°E basepoint. As can be seen in Figure 3(b), this same pattern can be traced back to lag day −6 near 50°E. From 25°E basepoint westward, WDCS convection is more enhanced at the trough region and slightly inside the southerlies. This pattern suggests that after the 25°E basepoint, the WDCS is weaker in terms of frequency, which coincides with the development of a strong easterly wave pattern.

Figure 4 demonstrates that WDCSs are dominant inside the southerly wave phase from 30° to 20°E and somewhat to the east of the trough axis area. The Darfur mountains are located in this area, and convection is initiated in association with presence of lower tropospheric moisture in southerlies. Therefore, it is not surprising that isolated and less well-organized convection represented by WDCSs are enhanced in association with the southerly anomalies. A strengthening of the easterly waves and MCSs is observed at 15°E and the weakening of WDCS commences in this region. As shown in Figure 4(a), the classical MCS-West African easterly wave characteristics are observed where there is strong enhanced convection in the vicinity of the trough and suppressed convection at the ridge. AEW strengthening at 10°E is observed along with enhancement of MCSs.

4. Discussion and remarks

This study uses a new ISCCP CS data set to explore the evolution of AEW convection across North Africa. The weaker AEWs over East Africa are primarily associated with WDCSs. As they intensify over Central Africa, MCSs become more prominent. We hypothesize that the AEW strengthening is associated with a simultaneous growth of synoptic scale MCS activity over Central Africa and also by an AEJ environment (the Central and East African region being the AEJ entrance).

WDCSs are generally enhanced in the southerly phase and suppressed in the northerly phase of the waves (Figures 2(b) and 3(b)). This pattern is stronger in Central and East Africa from 30° through 15°E (Figure 4(a)). MCSs are enhanced ahead of the trough westward of 25°E, consistent with previous studies (Berry and Thorncroft, 2005; Mekonnen *et al.*, 2006). By 10°E, the AEW structure is robust, consistent with its observed feature in West Africa (Reed *et al.*, 1977; Janiga and Thorncroft, 2016). This study confirms the relationship between AEWs and convection found in many past studies (e.g. Reed *et al.*, 1977; Janiga and Thorncroft, 2016). However, this study uniquely looks in greater detail at how that relationship evolves from AEW initiation in East Africa to maturity in West Africa. This evolution suggests a relationship between the development of MCSs and the strengthening of the AEWs over Central Africa. Overall, Figures 2–4 show that WDCSs over East Africa are enhanced in the AEW southerlies. Over West Africa, easterly waves have a strong relationship with enhanced MCSs at or ahead of the trough and suppressed MCS at or ahead of the ridge. Specifically, Figure 4 suggests that WDCSs propagate with the AEW southerlies between East and Central Africa, where enhanced MCS structures become prominent at and ahead of the trough. West of 20°E, the AEWs strengthened, but more evidence is needed to determine if this AEW strengthening is a potential response to increased convective heating by MCSs. Results suggest that the relationship between wave phases and different kinds of convection changes across tropical North Africa.

Figure 5 summarizes the relationship between AEW phases and deep convection over North Africa during a typical summer season. WDCSs are enhanced within the southerly anomalies to the west of an AEW ridge. They are most prevalent over eastern Africa and gradually recede in western Africa. WDCSs are particularly frequent near or just to the west of high terrain, indicating the important role

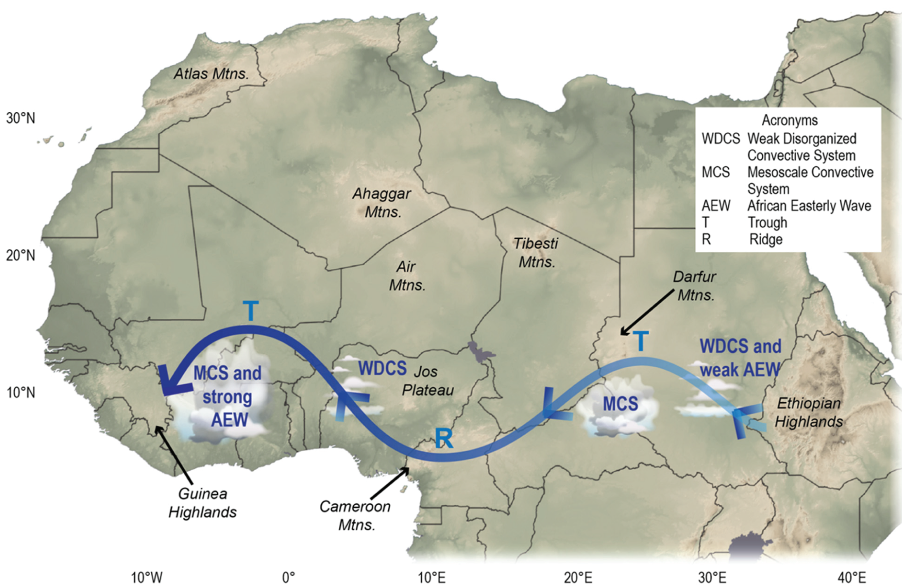

Figure 5. Schematic of AEWs and associated MCS and WDCS over a topographical map of northern Africa. Arrows were placed over areas of maximum northerlies and southerlies.

of the diurnal cycle in cloud organization. MCSs, on the other hand, are most common within the AEW northerly anomalies, consistent with Kiladis *et al.* (2006). Their frequency increase westwards from East Africa. Similar to WDCSs, MCS frequency increases near the Guinea Highlands, consistent with observations of Ventrice and Thorncroft (2013).

Mekonnen and Rossow (2011) speculated that the isolated and less well-organized convection from East Africa transitions into MCSs over Central Africa. The dynamic response to this increased diabatic heating is AEW initiation. This study supports this hypothesis using higher resolution CS data. This study provides new insights into how AEWs and convection interact over East Africa as suggested in past studies (Berry and Thorncroft, 2005; Mekonnen *et al.*, 2006; Thorncroft *et al.*, 2008; Mekonnen and Rossow, 2011). The current climatological study provides a unique perspective of how the mode of convection changes in association with easterly waves across tropical North Africa starting from the Ethiopian Highlands. Future in-depth analysis should consider more thermodynamic and dynamic factors at low and middle levels of the troposphere such as vertical shear, moisture flux convergence/divergence, convectively available potential energy and equivalent potential temperature to better understand how convection types interact with wave disturbances over the region.

Acknowledgements

This work is supported by NSF under grant no. AGS-1461911. Carl J. Schreck was supported by NOAA's Reference Environmental Data Record Program through the Cooperative Institute for Climate and Satellites – North Carolina under Cooperative Agreement NA14NES432003.

References

Berry GJ, Thorncroft C. 2005. Case study of an intense African easterly wave. *Mon. Weather Rev.* **133**: 752–766.

Burpee RW. 1972. The origin and structure of easterly waves in the lower troposphere of North Africa. *J. Atmos. Sci.* **29**: 77–90.

Carlson TN. 1969. Synoptic histories of three African disturbances that developed into Atlantic hurricanes. *Mon. Weather Rev.* **97**: 256–276.

Carvalho LMV, Jones C. 2001. A satellite method to identify structural properties of mesoscale convective systems based on the maximum spatial correlation tracking technique (MASCOTTE). *J. Appl. Meteorol.* **40**: 1683–1701.

Fink AH, Reiner A. 2003. Spatiotemporal variability of the relation between African easterly waves and West African squall lines in 1998 and 1999. *J. Geophys. Res. Atmos.* **108**(D11): 4332. https://doi.org/10.1029/2002JD002816.

Hall NMJ, Kiladis GN, Thorncroft CD. 2006. Three-dimensional structure and dynamics of African easterly waves. Part II: dynamical modes. *J. Atmos. Sci.* **63**: 2231–2245.

Hodges KI, Thorncroft CD. 1997. Distribution and statistics of African mesoscale convective weather systems based on the ISCCP Meteosat imagery. *Mon. Weather Rev.* **125**: 2821–2837.

Hsieh JS, Cook KH. 2005. Generation of African easterly wave disturbances: relationship to the African easterly jet. *Mon. Weather Rev.* **133**: 1311–1327.

Hsieh JS, Cook KH. 2007. A study of the energetics of African easterly waves using a regional climate model. *J. Atmos. Sci.* **64**: 421–440.

Hsieh JS, Cook KH. 2008. On the instability of the African easterly jet and the generation of African waves: reversals of the potential vorticity gradient. *J. Atmos. Sci.* **65**: 2130–2151.

Janiga MA, Thorncroft CD. 2013. Regional differences in the kinematic and thermodynamic structure of African easterly waves. *Q. J. R. Meteorol. Soc.* **139**: 1598–1614.

Janiga MA, Thorncroft CD. 2016. The influence of African easterly waves on convection over tropical Africa and the East Atlantic. *Mon. Weather Rev.* **144**: 171–192.

Kiladis GN, Thorncroft CD, Hall NMJ. 2006. Three-dimensional structure and dynamics of African easterly waves. Part I: observations. *J. Atmos. Sci.* **63**: 2212–2230.

Laing AG, Fritsch JM. 1993. Mesoscale convective complexes in Africa. *Mon. Weather Rev.* **121**: 2254–2263.

Lin YL, Robertson KE, Hill CM. 2005. Origin and propagation of a disturbance associated with an African easterly wave as a precursor of Hurricane Alberto (2000). *Mon. Weather Rev.* **133**: 3276–3298.

Machado LAT, Rossow WB. 1993. Structural characteristics and radiative properties of tropical cloud clusters. *Mon. Weather Rev.* **121**: 3234–3260.

Machado LAT, Rossow WB, Guedes RL, Walker AW. 1998. Life cycle variations of mesoscale convective systems over the Americas. *Mon. Weather Rev.* **126**: 1630–1654.

Maddox RA. 1980. Meoscale convective complexes. *Bull. Am. Meteorol. Soc.* **61**: 1374–1387.

Mathon V, Laurent H. 2001. Life cycle of Sahelian mesoscale convective cloud systems. *Q. J. R. Meteorol. Soc.* **127**: 377–406.

Mekonnen A, Rossow WB. 2011. The interaction between deep convection and easterly waves over tropical North Africa: a weather state perspective. *J. Clim.* **24**: 4276–4294.

Mekonnen A, Thorncroft CD, Aiyyer AR. 2006. Analysis of convection and its association with African easterly waves. *J. Clim.* **19**: 5405–5421.

Norquist DC, Recker EE, Reed RJ. 1977. The energetics of African wave disturbances as observed during phase III of GATE. *Mon. Weather Rev.* **105**: 334–342.

Novella NS, Thiaw WM. 2013. African rainfall climatology version 2 for famine early warning systems. *J. Appl. Meteorol. Climatol.* **52**: 588–606.

Oreopoulos L, Rossow WB. 2011. The cloud radiative effects of International Satellite Cloud Climatology Project weather states. *J. Geophys. Res. Atmos.* **116**: D12202. https://doi.org/10.1029/2010JD015472.

Reed RJ, Norquist DC, Recker EE. 1977. Structure and properties of African wave disturbances as observed during phase III of GATE. *Mon. Weather Rev.* **105**: 317–333.

Rossow WB, Schiffer RA. 1999. Advances in understanding clouds from ISCCP. *Bull. Am. Meteorol. Soc.* **80**: 2261–2287.

Rossow WB, Walker AW, Beuschel DE, Roiter MD. 1996. International Satellite Cloud Climatology Project (ISCCP) documentation of new cloud data sets, WMO/TD 737, 115 pp, World Meteorological Organization: Geneva.

Rossow WB, Tselioudis G, Polak A, Jakob C. 2005. Tropical climate described as a distribution of weather states indicated by distinct mesoscale cloud property mixtures. *Geophys. Res. Lett.* **32**: L21812. https://doi.org/10.1029/2005GL024584.

Rossow WB, Mekonnen A, Pearl C, Goncalves W. 2012. Tropical Precipitation Extremes. *J. Climate* **26**: 1457–1466.

Rossow WB, Mekonnen A, Pearl C, Goncalves W. 2013. Tropical precipitation extremes. *J. Clim.* **26**: 1457–1466.

Simmons A, Uppala S, Dee D, Kobayashi S. 2007. ERA-Interim: new ECMWF reanalysis products from 1989 onwards. *ECMWF Newsl.* **110**: 25–35.

Tan J, Jakob C, Lane TP. 2013. On the identification of the large-scale properties of tropical convection using cloud regimes. *J. Clim.* **26**: 6618–6632.

Thorncroft CD, Hoskins BJ. 1994. An idealized study of African easterly waves.1. A linear view. *Q. J. R. Meteorol. Soc.* **120**: 953–982.

Thorncroft CD, Hall NMJ, Kiladis GN. 2008. Three-dimensional structure and dynamics of African easterly waves. Part III: genesis. *J. Atmos. Sci.* **65**: 3596–3607.

Tromeur E, Rossow WB. 2010. Interaction of tropical deep convection with the large-scale circulation in the MJO. *J. Clim.* **23**: 1837–1853.

Ventrice MJ, Thorncroft CD. 2013. The role of convectively coupled atmospheric kelvin waves on African easterly wave activity. *Mon. Weather Rev.* **141**: 1910–1924.